Crystal Structures of Unliganded and Half-Liganded Human Hemoglobin Derivatives Cross-Linked between Lys 82β_1 and Lys 82β_2[‡]

Sam-Yong Park,[§] Naoya Shibayama,[||] Toshiki Hiraki,[§] and Jeremy R. H. Tame*[,§]

Protein Design Laboratory, Graduate School of Integrated Science, Yokohama City University, 1-7-29 Suehiro, Tsurumi, Yokohama 230-0045, Japan, and Department of Physiology, Division of Biophysics, Jichi Medical School, 3311-1 Yakushiji, Minamikawachi, Kawachi, Tochigi 329-0498, Japan

Received January 9, 2004; Revised Manuscript Received April 12, 2004

ABSTRACT: A number of ligand binding studies of human adult hemoglobin (HbA) cross-linked between Lys 82β_1 and Lys 82β_2 with bis(3,5-dibromosalicyl)fumarate have been reported. The oxygen binding properties of native HbA, including the cooperativity and Bohr effect, are not substantially changed by the modification, provided care is taken to remove electrophoretically silent impurities arising from side reactions. We have refined the high-resolution structure of this modified Hb and found it adopts the T state when crystallized in the absence of heme ligands, contrary to a previously published structure. These results suggest the slightly altered crystal form determined previously may be due to unremoved side products of the cross-linking reaction with high oxygen affinity. Two nickel-substituted Hbs cross-linked in the same way have also been crystallized in the presence of carbon monoxide, which binds only to the ferrous heme. In the case of the nickel-substituted α subunit, the absence of a covalent link between the central metal of the heme and the proximal histidine leads to a new conformation of the histidine stabilized by a water molecule. This structure may mimic that of partially NO-liganded species of HbA; however, overall, the changes are highly localized, and both doubly ligated species are in the T conformation.

Despite decades of study, the allosteric mechanism of human hemoglobin remains a cause of debate, from both a structural and thermodynamic point of view. Considerable controversy has surrounded the two-state model proposed by Perutz (*1*) in which he identified the structures of unliganded Hb[1] and liganded Hb with the tense (T) and relaxed (R) states of the Monod−Wyman−Changeux allosteric model (*2*). Perutz reviewed the structural evidence for his model 28 years later and found it to have survived largely intact (*3*). While the two-state model can be fitted very well to the oxygen binding properties of Hb under fixed solution conditions, it is clear that ligation intermediates carrying one, two, or three ligands must exist. To discover the nature of key intermediates on the allosteric pathway, numerous crystal studies have been undertaken to determine the structure of partially liganded Hbs (*4*, *5*) or Hbs restrained by cross-links (*6*, *7*) or the crystal lattice (*8*). Crystal structures, however, are unable to give a precise or accurate indication of the free energy of the molecular species they represent, and other biophysical methods are required to determine the relative importance of particular states. Smith and Ackers (*9*) used a deoxy-cyanomet hybrid system to model Hb with oxygen at particular hemes within the tetramer, ligand binding being assessed through its coupling to the dimer−tetramer equilibrium of Hb. In this way, Ackers and colleagues measured the stability of all possible different ligation intermediates (*10*, *11*). Perrella and co-workers have approached the same problem of measuring the concentrations of intermediates on the ligation pathway by the rapid quenching of the reaction between Hb and CO. Cryogenic isoelectric focusing was used to quantitate the amounts of each intermediate, showing a marked asymmetry in the ligation pathway (*12*, *13*). Experiments by Shibayama used nickel hybrid Hbs to measure the affinity of ferrous hemes within the tetramer, the nickel-substituted hemes being unable to bind oxygen or CO (*14*, *15*). A chemical cross-link was used in these experiments to ensure that the asymmetrically substituted tetramers did not dissociate into dimers, which would permit them to form a mixture of differently substituted molecules. The cross-linking reagent used was bis(3,5-dibromosalicyl)-fumarate, a frequently studied reagent which specifically links the two β subunits via Lys 82. This reagent links the protein symmetrically, across the molecular 2-fold axis, at the site of 2,3-diphosphoglycerate (DPG) binding. We use the name XL82β-Hb to describe native human Hb cross-linked in this way. Other researchers have also used the same reagent to prepare asymmetrically modified Hbs (*16*−*18*).

The oxygen binding properties and X-ray structure of XL82β-Hb were first reported in 1980 (*19*). At 4.4 Å resolution, the cross-link was found to cause only minor perturbations in the deoxy form, though the oxygen affinity was reported to be high, and cooperativity was reduced compared to that of HbA. Significant changes in the oxygen binding curve were also reported in 1987 (*17*). Shibayama

[‡] Coordinates have been deposited in the Protein Data Bank as entries 1UIW, 1J3Z, and 1J40.

* To whom correspondence should be addressed. Telephone: +81-45-508-7228. Fax: +81-45-508-7366. E-mail: jtame@tsurumi.yokohama-cu.ac.jp.

[§] Yokohama City University.

[||] Jichi Medical School.

[1] Abbreviations: Hb, hemoglobin; HbA, human adult Hb; XL82β-Hb, HbA cross-linked with bis(3,5-dibromosalicyl) fumarate.

10.1021/bi049932w CCC: $27.50
Published on Web 06/15/2004

and co-workers (*20*), however, found that the reported preparation protocols produced samples containing roughly 20% of a chromatographically silent side product. This impurity was detected and removed by utilizing the greatly increased reactivity of its sulfhydryl group at cysteine 93β. Removal of the impurity yields a cross-linked Hb which exhibited oxygen binding characteristics much closer to those of HbA than originally reported. Recently, the crystal structure of deoxy XL82β-Hb was refined to 2.3 Å resolution (*21*) and reported to be intermediate between the R and T states of HbA. Since the sample was purified simply by ion-exchange chromatography without regard to isoelectric side products, however, it presumably contained high-oxygen affinity impurities. We have determined the X-ray structure of deoxy XL82β-Hb purified for removal of such side products and refined it to 1.5 Å resolution. The protein adopts the T quaternary structure, consistent with the oxygen binding curves of this chemically modified protein reported previously (*20*).

We have also refined the structures of two asymmetric nickel hybrid Hbs cross-linked and purified in the same way. In these hybrid molecules, either the α subunits or the β subunits contain hemes carrying nickel instead of iron. These high-resolution structures extend the conclusions drawn earlier from similar metal hybrid Hb models, and show how Hb in the T state responds to ligation at the α or β hemes.

EXPERIMENTAL PROCEDURES

Preparation of Cross-Linked Hemoglobin. Bis(3,5-dibromosalicyl)fumarate was synthesized according to the method of Walder (*22*) and recrystallized twice from ethanol. HbA was prepared and cross-linked with bis(3,5-dibromosalicyl)fumarate under CO to produce XL82β-HbA as described previously (*20*). The purification of the XL82β-HbA product was also carried out according to the method developed by Shibayama et al. (*20*). Isoelectric impurities were removed by utilizing a difference between the desired product and the impurities in the reactivity of the sulfhydryl groups of Cys 93β toward *N*-ethylmaleimide under deoxy conditions. Cross-linked iron(II)−nickel(II) hybrid Hbs, XL82β-[α(Fe−CO)β(Ni)]$_2$ and XL82β-[α(Ni)β(Fe−CO)]$_2$, were prepared and purified as described previously (*15*).

Crystallization and Structure Determination. Crystallization of the cross-linked iron(II)−nickel(II) hybrid Hbs has been described elsewhere (*23*). Crystallization of deoxy XL82β-HbA was carried out in a deoxygenated solution of 1% Hb, 10% PEG-6000, 100 mM potassium chloride, 10 mM potassium phosphate (pH 7.0), and 5 mM sodium dithionite by the batch method. The crystals belong to monoclinic space group *P*21 and contain two molecules per asymmetric unit, with the following unit cell dimensions: $a = 66.14$ Å, $b = 96.34$ Å, $c = 102.48$ Å, and $\beta = 101.79°$. Crystals were mounted in a fiber loop under air using dithionite to prevent oxygenation (*24*), and cooled using a 100 K nitrogen gas stream. Glycerol (150 μL/mL) was added to the mother liquor to avoid the formation of ice or crystal damage upon cryocooling. High-resolution diffraction data were obtained using synchrotron radiation at RIKEN beam line BL44B2 (RIKEN Structural Biology Beamline II) of SPring-8 (Harima, Japan). Intensity data were collected with a MAR CCD detector. The wavelength of the incident X-rays was 1.0 Å. All diffraction data were integrated and scaled with HKL2000 and SCALEPACK (*25*). The initial models of XL-Hb and HbCO were obtained by molecular replacement using MOLREP. The models were improved by a cyclic procedure of model building using TURBO (*26*) and refinement using REFMAC. Both REFMAC and MOLREP are part of the CCP4 suite (*27*). The crystallographic and refinement data are summarized in Table 1. The model has been deposited in the Protein Data Bank as entry 1UIW.

Table 1: Crystal Parameters, Data Collection, and Structure Refinement Statistics of Deoxy XL82β Hb[a]

space group	$P2_1$
cell dimensions	$a = 66.14$ Å, $b = 96.34$ Å, $c = 102.48$ Å, $\beta = 101.79°$
resolution range (Å)	29.0−1.50
no. of measured reflections	684867
no. of unique reflections	182747
completeness (overall/outer shell) (%)	95.6/74.3
mean $\langle I\rangle/\langle\sigma(I)\rangle$ (overall)	16.5
multiplicity (overall)	3.7
R_{merge} (overall/outer shell) (%)[b]	4.8/17.6
refinement statistics	
resolution range (Å)	29.0−1.5
R-factor (%)[c]	17.2
R_{free} (%)[d]	20.5
no. of water molecules	870
rms deviations from ideal values	
bond lengths (Å)	0.017
bond angles (deg)	1.562
Ramachandran plot	
residues in most favorable regions (%)	93.4
residues in additional allowed regions (%)	6.4

[a] The outer shell has resolution limits of 1.50−1.55 Å. The structures of XL[α(Fe−CO)β(Ni)]$_2$ and XL[α(Ni)β(Fe−CO)]$_2$ were reported previously (*23*) (PDB entries 1J3Z and 1J40). [b] $R_{merge} = \sum|I_i - \langle I\rangle|/\sum|I_i|$, where I_i is the intensity of an observation and $\langle I\rangle$ in the mean value for that reflection and the summations are over all reflections. [c] *R*-factor $= \sum_h||F_o(h)| - |F_c(h)||\sum_h F_o(h)$, where F_o and F_c are the observed and calculated structure factor amplitudes, respectively. No σ cutoff was applied. [d] R_{free} was calculated with 5% of the data omitted from the refinement.

RESULTS

Structure of Cross-Linked Native Human Hb. The structure of deoxy XL82β-Hb cryocooled to 100 K was determined and refined to 1.5 Å resolution. The quality of the electron density map is shown in Figure 1; the cross-link is clearly visible in the $2F_o - F_c$ density map. This constrasts strongly with the structure of horse Hb locked in the R state by bis(*N*-maleimidoethyl) ether (BME) in which the chemical cross-link proved to be invisible in the electron density maps (*7*). Unlike the previously reported model of deoxy XL82β-Hb [PDB entry 1BIJ (*21*)], we find no trace of a water molecule hydrogen bonded to the amide linkages of the fumaryl moiety. Figure 2 shows the Cα trace of the $\alpha_1\beta_1$ dimer superimposed on that of native deoxy Hb at 120 K (*24*). The rms deviation of the Cα atoms shows the structure to be very close to the normal T state of unmodified human Hb (Table 2).

The cross-linked Hb retains the usual features of the T state, including the hydrogen bond between Tyr 42α_1 and Asp 99β_2 which gives rise to a line in NMR spectra

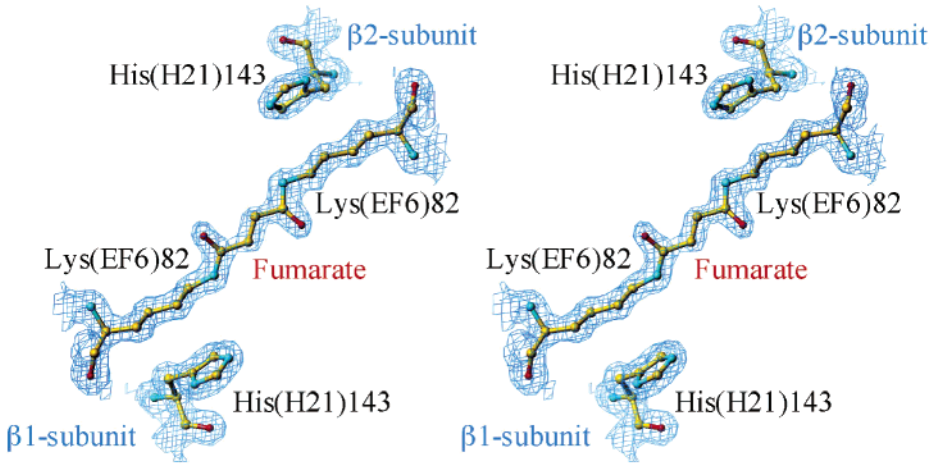

FIGURE 1: Stereoview of the $2F_o - F_c$ electron density map covering the chemical cross-link in one Hb tetramer in the asymmetric unit. The map is contoured at 1.3σ.

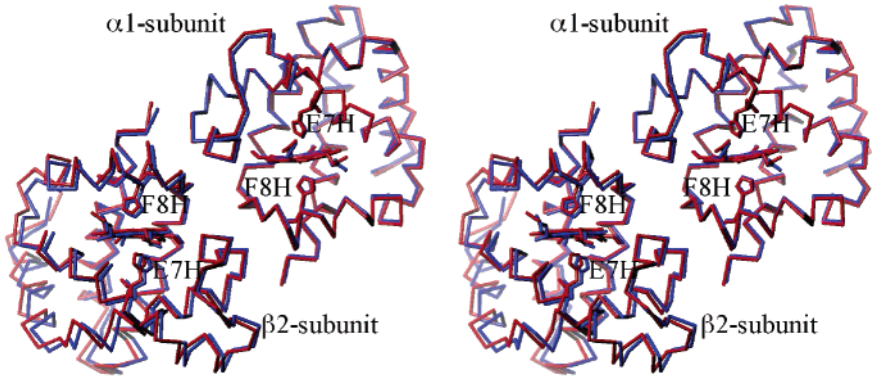

FIGURE 2: Stereoview of a least-squares superposition of XL82β-Hb (red) and deoxy HbA (blue), showing the α_1 and β_2 subunits after overlapping the Cα atoms of the $\alpha_1\beta_1$ dimers. The similarity of the overall structure is seen from the close resulting fit of the $\alpha_1\beta_2$ interface which changes when the compound switches between quaternary states.

Table 2

Cα Atom rms Deviations within the Asymmetric Unit of Various Deoxy Hb Structures

	HbA[a]	XL82β-Hb[b]	1BIJ	no. of atoms
α subunits	0.31	0.20	1.76[c]	141
β subunits	0.25	0.43	0.67	145
αβ dimers	0.32	0.42	1.37	286

Cα Atom rms Deviations of Deoxy HbA[a] from Deoxy-Cross-Linked Hb Tetramers

XL82β-Hb	XL[α(Ni)β(Fe−CO)]$_2$	XL[α(Fe−CO)β(Ni)]$_2$	1BIJ
0.63	0.73	0.76	1.07

[a] HbA here refers to PDB entry 1A3N. This structure has no 1β residue modeled, so this residue has been omitted from all calculations. [b] Distances calculated using chains A−D of the structure (PDB entry 1UIW). [c] The large deviation seen between the two copies of the α chain in 1BIJ is due to the partial unfolding of helix F in one subunit.

characteristic of the T state (*28*). The C-termini of both the α and β chains also form interactions found in T but not R state Hb, with the exception of the C-terminal histidine of one copy of the four β chains in the asymmetric unit. In deoxy Hb, this histidine normally forms a salt bridge with Asp 94 of the same chain. Crystal contacts appear to disturb this interaction in one case (Table 3). Since the Bohr effect (pH dependence of oxygen affinity) of XL82β-Hb is very similar to that of HbA (*20*), it is probable this interaction is not disturbed by the cross-link in solution. The list of interactions characteristic of the T state given in Table 3 indicates deoxy XL82β-Hb adopts a T state conformation.

Structure of Cross-Linked Nickel Hybrid Hbs. Since nickel is unable to bind oxygen or carbon monoxide, nickel hybrids of XL82β-Hb have previously been used as models of Hb with deoxyferrous hemes (*15*, *20*). The crystal structures of these hybrids have been refined to high resolution in the CO-bound form, and are found to show qualitative agreement with the lower-resolution refinements of partially liganded Hbs carried out previously (*4*, *5*). The structures of XL82β-[α(Ni)β(Fe−CO)]$_2$ and XL82β-[α(Fe−CO)β(Ni)]$_2$ are deposited in the Protein Data Bank as entries 1J40 and 1J3Z, respectively. We have previously described the changes in these structures on photolysis of the Fe−CO bond with a laser (*23*). XL82β-Hb and the two forms of cross-linked Hb all gave crystals in space group $P2_1$ with similar cell lengths and containing two Hb tetramers per asymmetric unit. The small differences in the unit cell measurements are probably due to slight differences in the pH of crystallization (pH 6.6 for the hybrids and pH 7.0 for the native structure). Electron density covering the α heme of both hybrid structures is shown in Figure 3. Like deoxy XL82β-Hb, the two hybrids with nickel replacing iron in the α and β subunits also adopt the T structure, even in the presence of CO which binds to the subunits with ferrous hemes. Replacing iron with nickel in the α subunit gives rise to a slightly altered tertiary structure in which the bond between the heme metal and the proximal histidine is broken. In the liganded T state, this

Table 3: Distances Characteristic of the T State[a]

	deoxy HbA		XL82β-Hb		HbCO	1BIJ	
Lys 40α_1 Nζ−His 146β_2 O	2.73	2.70	2.64 2.78	2.85 2.85	>15	3.17	2.92
Asp 94β_1 Oϵ_1−His 146β_1 Nϵ_1	2.69	2.80	2.89 9.76	3.36 2.78	>11	2.78	3.42
Tyr 42α_1 Oη−Asp 99β_2 Oδ_2	2.59	2.51	2.67 2.67	2.67 2.68	>7	3.26	2.72
Asp 94α_1 Oδ_2−Trp 37β_2 Nϵ_1	2.90	2.87	2.96 3.04	3.02 3.01	3.66	3.04	2.93
Asp 94α_1 Oδ_2−Asn 102β_2 Nδ_1	>4	>4	>4 >4	>4 >4	2.74	>4	2.82

[a] The number of distances given for each structure reflects the number of molecules in the asymmetric unit. All distances are given in angstroms. Deoxy HbA is PDB entry 1A3N, and HbCO is PDB entry 1IRD.

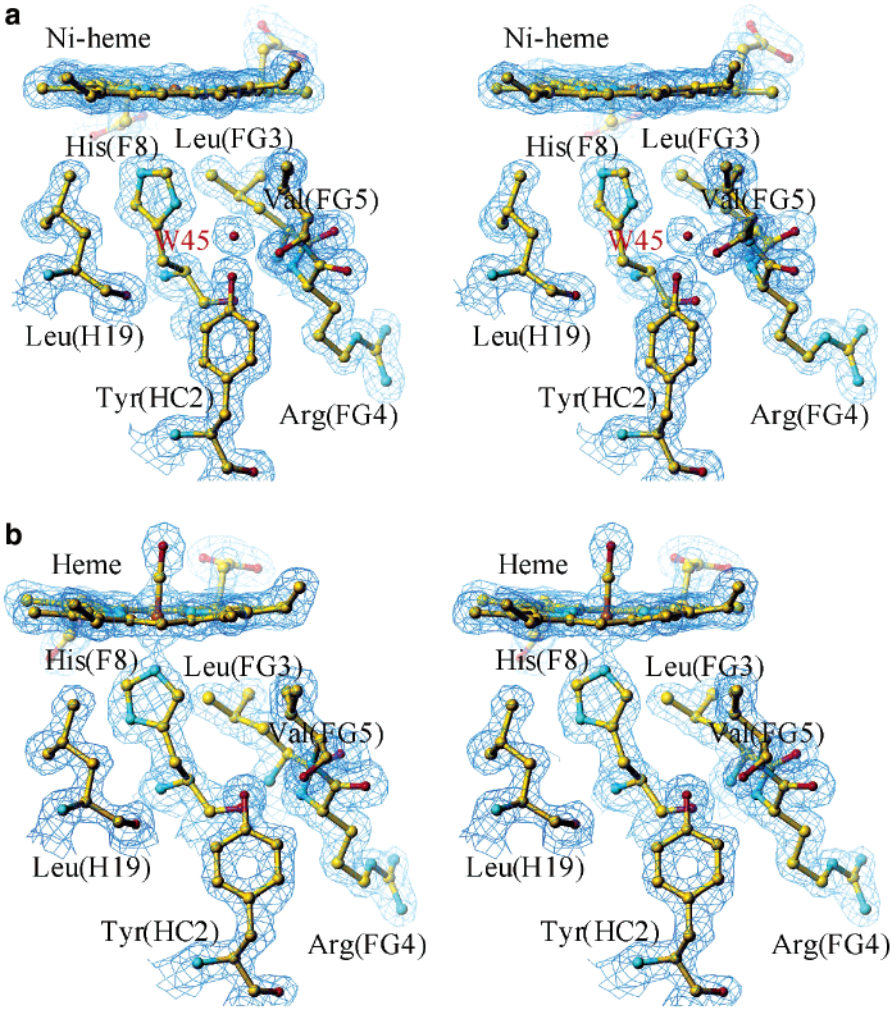

FIGURE 3: (a) Electron density map ($2F_o - F_c$) covering the nickel-substituted α heme in XL82β-[α(Ni)β(Fe−CO)]$_2$, contoured at 1.3σ. The nickel is four-coordinate and the heme planar, allowing the proximal histidine to rotate its imidazole side chain to create a binding site for water. The interactions formed by this water molecule are shown in Figure 4. (b) Equivalent view of the ferrous, carbon monoxy α heme in XL82β-[α(Fe−CO)β(Ni)]$_2$, contoured at 1.3σ. The heme is close to planar, but the bond to the proximal histidine is intact. No water molecule is seen close to histidine F8, even at low contour levels.

bond is under tension, much more than the equivalent bond in the β subunits (*8*, *29*). Freed of this restraining link, the α subunit proximal histidine in the XL82β-[α(Ni)β(Fe−CO)]$_2$ structure moves to hydrogen bond to a novel water molecule which appears in the electron density map (Figure 3). This water molecule presumably stabilizes the proximal histidine in its new conformation, since it is not seen in other Hb structures, including XL82β-[α(Fe−CO)β(Ni)]$_2$ in which the iron−histidine bond is intact. A schematic diagram showing the interactions formed by the new water molecule is given in Figure 4. Overall, the conformation of the α chain is altered little by the breakage of the heme−histidine bond, and no major movements are required to create the new water binding site. One key difference is the failure to form a direct hydrogen bond between Asp 94α_1 and Trp 37β_2 which is a usual hallmark of the T state. The tertiary structure of the α chain is slightly changed around the F−G corner, allowing the new water molecule to enter between these residues, but otherwise, the α chains of the two nickel hybrids overlap closely (Figure 5). The β chain, however, is found in its T

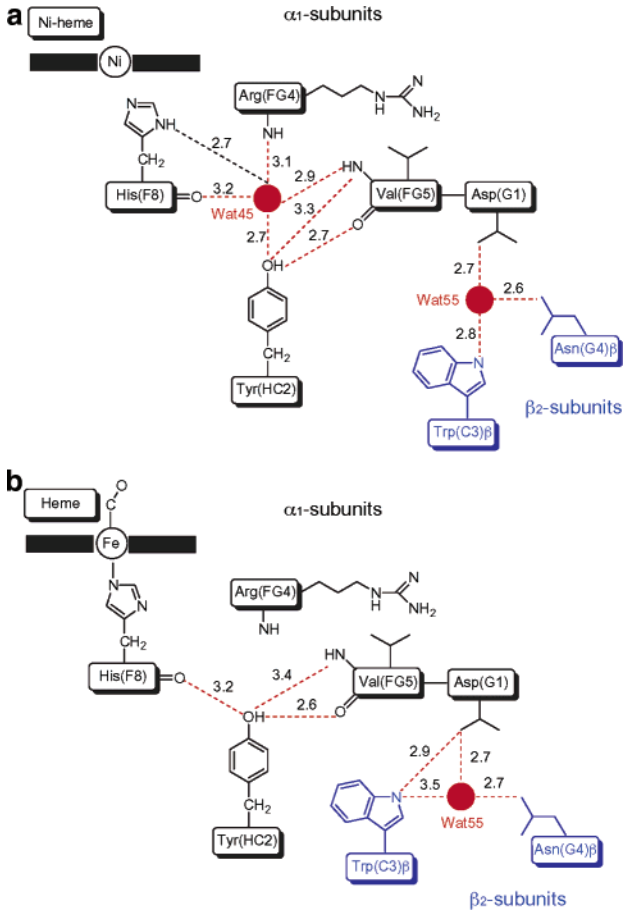

FIGURE 4: (a) Schematic diagram showing the interactions formed by the water molecules introduced close to the α heme on rupture of the heme−histidine bond in XL82β-[α(Ni)β(Fe−CO)]$_2$. All distances are given in angstroms. Even at 1.5 Å resolution, the hydrogen atoms in the structure are not visible, and the diagram is not intended to imply any particular protonation state of any group. (b) Equivalent diagram of the interactions found in the ligated ferrous heme of XL82β-[α(Fe−CO)β(Ni)]$_2$, showing the usual pattern of hydrogen bonding found in T state Hb.

state tertiary structure, forming the hydrogen bond between Asp 94 and His 146 which is also used as a marker for the T state. The Asp 94α_1−Asn 102β_2 hydrogen bond, a marker for the R state, is not formed.

Comparison of the two nickel hybrid structures described here underlines the very different control of heme reactivity operating in the α and β subunits. Since the β heme metal moves less on the R−T transition, the nickel atoms in XL82β-[α(Fe−CO)β(Ni)]$_2$ remain five-coordinate in the T state, but those of XL82β-[α(Ni)β(Fe−CO)]$_2$ are four-coordinate. Szabo and Perutz showed in 1976 that when NO-liganded Hb is forced into the T state by the addition of IHP, the bonds between the proximal histidines and the α chain hemes break, while the equivalent bonds in the β chains are left intact (*30*). The physiological relevance of this experiment was unknown at the time. NO is an important natural regulator of vascular tone and binds strongly to heme (*31*). Limited NO binding to Hb results in the formation of α-nitrosyl Hb [α(Fe−NO)β(Fe)]$_2$, which has low oxygen affinity but exhibits the R−T allosteric transition, cooperative ligand binding to the β hemes, and a Bohr effect comparable to that of HbA (*32*). Since NO binding greatly weakens the iron bond to the proximal histidine, the structure of the α-(Ni) subunits in XL82β-[α(Ni)β(Fe−CO)]$_2$ may mimic the α subunits of [α(Fe−NO)β(Fe)]$_2$. Two new water molecules introduced into the structure appear to stabilize the altered conformations of side chains around the F−G corner (Figure 4a). α-Nitrosyl Hb is cooperative, however, and must switch to a high-affinity state upon ligation of the β hemes, whereas XL82β-[α(Ni)β(Fe−CO)]$_2$ maintains the T state.

The structures of the nickel hybrid structures also clarify experiments carried out on recombinant Hbs with the proximal histidines replaced with glycine. In the presence of imidazole, these proteins behave as normal Hb but with severed bonds between the side chain and main chain of the proximal histidine, releasing any tension at the heme (*33*). It was found that, in the presence of CO bound to all four hemes, releasing tension in the α subunits led to considerable T structure, but releasing tension in the β chains did not. Releasing tension in both led to an intermediate between the two. This shows that the position of the β heme iron is relatively insensitive to quaternary state, and distal effects are more important in this subunit. rHbCO (αH87G) is held in the T state by the α chain freed of the pull of the heme iron; the additional mutation in rHbCO (αH87G/βH92G) allows the β heme to move more in response to distal ligand,

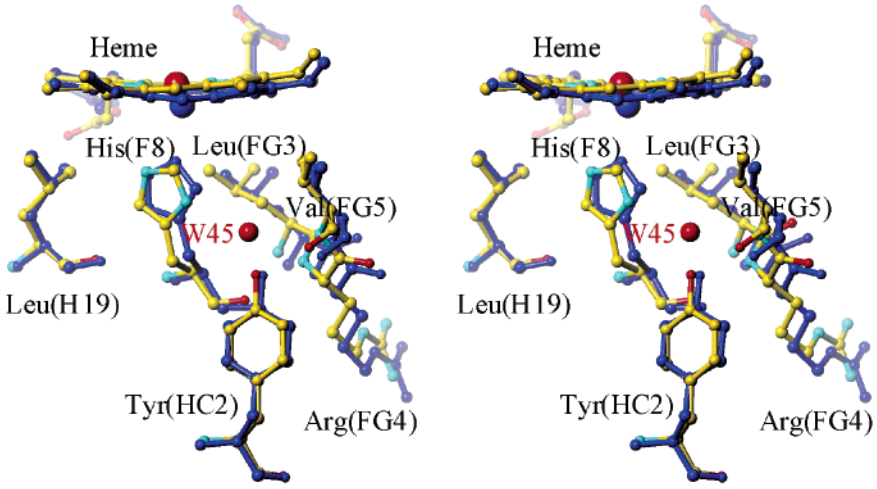

FIGURE 5: Overlay of the proximal region of the α hemes in XL82β-[α(Ni)β(Fe−CO)]$_2$ and XL82β-[α(Fe−CO)β(Ni)]$_2$ (shown in blue). The extra water molecule introduced close to the proximal histidine in XL82β-[α(Ni)β(Fe−CO)]$_2$ is shown in red. Replacement of the iron with nickel relaxes the heme, which flattens, allowing the F−G corner to follow its movement away from the histidine.

leading to a smaller value of *L*, the allosteric equilibrium constant ([T]/[R]). rHbCO (βH92G) is fully R state since the α subunit iron is pulled close to the heme, and the ligated heme in the β subunit is more free to move away from Val E11. The structures of XL82β-[α(Ni)β(Fe−CO)]$_2$ and XL82β-[α(Fe−CO)β(Ni)]$_2$ show that ligation of either subunit type is compatible with the T state (*4*, *5*), but tension builds on the proximal side of the liganded α heme and the distal side of the liganded β heme. This result is entirely consistent with previous oxygen binding and NMR analysis of Hb in which the iron is removed from either the α or β subunit, breaking the heme−protein linkage (*34*).

DISCUSSION

In agreement with our results presented here, previous models of partially liganded Hbs suggest that appreciable conformational flexibility may be found within the T state, while preserving key interactions at the $\alpha_1\beta_2$ interface (*35*). The structure of XL82β-[α(Ni)β(Fe−CO)]$_2$ shows how both liganded β hemes and planar α hemes can be fitted into the T quaternary state by decoupling the α subunit proximal histidines from the heme metal. Clearly, different structures are compatible with the presence of the "T state marker" resonances observed in NMR spectra. Further evidence of tertiary plasticity within the T state has recently emerged from combined oxygen equilibrium and spectroscopic studies of half-liganded zinc hybrid Hb (*36*).

Upon switching between the R and T states, one αβ dimer rotates relative to the other by ∼15° (*37*). Using the oxy and deoxy structures refined by Shaanan (*38*) and Fermi (*39*), Fernandez and co-workers suggested that overlapping the BGH frame of $\alpha_1\beta_1$ with 1BIJ shows the cross-linked structure to have a dimer rotation intermediate between the R and T states (*21*). The rotation from the T state was found to be ∼3°. Using nearly all Cα atoms, we find the dimer rotation between 1BIJ and these structures to be 13.0° and 2.1°. The direction cosines for the rotation are rather different however, the two axes of rotation making an angle of 81°, close to a random orientation (90°). Using the structure of HbCO determined using a cryocooled crystal (PDB entry 1IRD), it is found that 1BIJ shows a dimer rotation of more than 14°. The cross-linked structures are most similar in terms of the angle of rotation, but overall, there is little indication from 1BIJ or our refinement of deoxy XL82β-Hb that the cross-link impedes the quaternary transition.

During the R to T transition of native human Hb, the β chains move ∼4 Å further apart, opening the central cavity. Fernandez and co-workers (*21*) suggested that the fumaryl cross-link of 1BIJ pulls the β chains closer together and affects their movements significantly, the E helix and E−F corner being the most perturbed parts of the structure. Cys 93β was found to be in the T state conformation, but Tyr 145β does not take up its usual T state position in a cleft between the F and H helices. Overall, the β subunits were reported to be more strongly affected than the α subunits and the β residues near the cross-link to be much more affected than other parts of the structure. Our analysis of 1BIJ, however, shows the N-terminal turns of the α helix F to be completely unfolded, giving a large rms deviation in the overlapping of the two copies of the α chain in the asymmetric unit (Table 2). We do not see significant movements of the β chain E helix or E−F corner in our refined structure or 1BIJ. Our refinement of deoxy XL82β-Hb shows all the interactions expected of T state Hb (Table 3).

CONCLUSIONS

The high-resolution structures of native and nickel hybrid Hbs described here show that the chemical cross-link between the β subunits does not restrain the protein from adopting the T state characteristic of deoxy human Hb. This result agrees with the oxygen equilibrium studies carried out more than a decade ago, and more recent work with the symmetric and asymmetric nickel-substituted Hbs (*15*, *20*). The crystal structure of XL82β-Hb described previously (*21*) shows the tetramer adopts a slightly altered quaternary structure which retains many hallmark features of the T state. The unusual deviations from noncrystallographic symmetry, however, suggest some problems with this refinement at 2.3 Å resolution. Other oxygen binding studies of XL82β-Hb prepared as described by Fernandez and co-workers show reduced cooperativity and increased ligand affinity. This result may be expected if side reactions by the cross-linking reagent have modified other groups on the protein. Since the cross-linking was applied to liganded Hb, these side products may well be impeded from switching fully to the T state. Our X-ray results show that, with additional purification, deoxy XL82β-Hb adopts the T state quaternary structure. This has allowed us recently to use these modified Hbs to grow stable T state crystals for photolysis studies, and examine the tertiary structure changes as α and β subunits of T state Hb bind or lose the ligand (*23*).

REFERENCES

1. Perutz, M. F. (1970) Stereochemistry of cooperative effects in haemoglobin, *Nature 228*, 726−739.
2. Monod, J., Wyman, J., and Changeuz, J.-P. (1965) On the nature of allosteric transitions: a plausible model, *J. Mol. Biol. 12*, 88−118.
3. Perutz, M. F., Wilkinson, A. J., Paoli, M., and Dodson, G. G. (1998) The stereochemical mechanism of the cooperative effects in hemoglobin revisited, *Annu. Rev. Biophys. Biomol. Struct. 27*, 1−34.
4. Luisi, B., and Shibayama, N. (1989) Structure of haemoglobin in the deoxy quaternary state with ligand bound at the α haems, *J. Mol. Biol. 206*, 723−736.
5. Luisi, B., Liddington, B., Fermi, G., and Shibayama, N. (1990) Structure of deoxy-quaternary haemoglobin with liganded β subunits, *J. Mol. Biol. 214*, 7−14.
6. Schumacher, M. A., Dixon, M. M., Kluger, R., Jones, R. T., and Brennan, R. G. (1995) Allosteric transition intermediates modelled by crosslinked haemoglobins, *Nature 375*, 84−87.
7. Wilson, J., Phillips, K., and Luisi, B. (1996) The crystal structure of horse deoxyhaemoglobin trapped in the high-affinity (R) state, *J. Mol. Biol. 264*, 743−756.
8. Paoli, M., Liddington, R., Tame, J., Wilkinson, A., and Dodson, G. (1996) Crystal structure of T state haemoglobin with oxygen bound at all four haems, *J. Mol. Biol. 256*, 775−792.
9. Smith, F. R., and Ackers, G. K. (1985) Experimental resolution of cooperative free energies for the ten ligation states of human hemoglobin, *Proc. Natl. Acad. Sci. U.S.A. 82*, 5347−5351.
10. Ackers, G. K., Doyle, M. L., Myers, D., and Daugherty, M. A. (1992) Molecular code for cooperativity in hemoglobin, *Science 255*, 54−63.
11. Ackers, G. K., Perrella, M., Holt, J. M., Denisov, I., and Huang, Y. (1997) Thermodynamic stability of the asymmetric doubly-ligated hemoglobin tetramer (α+CNβ+CN)(αβ): methodological and mechanistic issues, *Biochemistry 36*, 10822−10829.

12. Perrella, M., and Di Cera, E. (1999) CO ligation intermediates and the mechanism of hemoglobin cooperativity, *J. Biol. Chem. 274*, 2605−2608.
13. Perrella, M., Benazzi, L., Shea, M. A., and Ackers, G. K. (1990) Subunit hybridization studies of partially ligated cyanomethemoglobins using a cryogenic method. Evidence for three allosteric states, *Biophys. Chem. 35*, 97−103.
14. Shibayama, N., Imai, K., Morimoto, H., and Saigo, S. (1993) Oxygen equilibrium properties of asymmetric nickel(II)-iron(II) hybrid hemoglobin, *Biochemistry 32*, 8792−8798.
15. Shibayama, N., Imai, K., Morimoto, H., and Saigo, S. (1995) Oxygen equilibrium properties of nickel(II)-iron(II) hybrid hemoglobins cross-linked between 82 β_1 and 82 β_2 lysyl residues by bis(3,5-dibromosalicyl)fumarate: determination of the first two-step microscopic Adair constants for human hemoglobin, *Biochemistry 34*, 4773−4780.
16. Miura, S., and Ho, C. (1984) Proton nuclear magnetic resonance investigation of cross-linked asymmetrically modified hemoglobins: influence of the salt bridges on tertiary and quaternary structures of hemoglobin, *Biochemistry 23*, 2492−2499.
17. Miura, S., Ikeda-Saito, M., Yonetani, T., and Ho, C. (1987) Oxygen equilibrium studies of cross-linked asymmetrical cyanomet valency hybrid hemoglobins: models for partially oxygenated species, *Biochemistry 26*, 2149−2155.
18. Kitagishi, K., D'Ambrosio, C., and Yonetani, T. (1988) Electron paramagnetic resonance study on crosslinked asymmetric Fe(II)-Co(II) hybrids of hemoglobin, *Arch. Biochem. Biophys. 264*, 176−183.
19. Walder, J. A., Walder, R. Y., and Arnone, A. (1980) Development of antisickling compounds that chemically modify hemoglobin S specifically within the 2,3-diphosphoglycerate binding site, *J. Mol. Biol. 141*, 195−216.
20. Shibayama, N., Imai, K., Hirata, H., Hiraiwa, H., Morimoto, H., and Saigo, S. (1991) Oxygen equilibrium properties of highly purified human adult hemoglobin cross-linked between 82 β_1 and 82 β_2 lysyl residues by bis(3,5-dibromosalicyl) fumarate, *Biochemistry 30*, 8158−8165.
21. Fernandez, E. J., Abad-Zapatero, C., and Olsen, K. W. (2000) Crystal structure of Lys β(1)82-Lys β(2)82 crosslinked hemoglobin: a possible allosteric intermediate, *J. Mol. Biol. 296*, 1245−1256.
22. Walder, J. A., Zaugg, R. H., Walder, R. Y., Steele, J. M., and Klotz, I. M. (1979) Diaspirins that cross-link β chains of hemoglobin: bis(3,5-dibromosalicyl) succinate and bis(3,5-dibromosalicyl) fumarate, *Biochemistry 18*, 4265−4270.
23. Adachi, S., Park, S. Y., Tame, J. R. H., Shiro, Y., and Shibayama, N. (2003) Direct observation of photolysis-induced tertiary structural changes in hemoglobin, *Proc. Natl. Acad. Sci. U.S.A. 100*, 7039−7044.
24. Tame, J. R. H., and Vallone, B. (2000) The structures of deoxy human haemoglobin and the mutant Hb Tyr α42 His at 120 K, *Acta Crystallogr. D56*, 805−811.
25. Otwinowski, Z., and Minor, W. (1997) Processing of X-ray diffraction data collected in oscillation mode, *Methods Enzymol. 276*, 307−326.
26. Roussel, A., and Cambillau, C. (1989) *TURBO*, pp 77−78, Silicon Graphics, Mountain View, CA.
27. Collaborative Computational Project No. 4 (1994) *Acta Crystallogr. D50*, 760−763.
28. Ho, C. (1992) Proton nuclear magnetic resonance studies on hemoglobin: cooperative interactions and partially ligated intermediates, *Adv. Protein Chem. 43*, 153−312.
29. Paoli, M., Dodson, G., Liddington, R. C., and Wilkinson, A. J. (1997) Tension in haemoglobin revealed by Fe−His(F8) bond rupture in the fully liganded T-state, *J. Mol. Biol. 271*, 161−167.
30. Szabo, A., and Perutz, M. F. (1976) Equilibrium between six- and five-coordinated hemes in nitrosylhemoglobin: interpretation of electron spin resonance spectra, *Biochemistry 15*, 4427−4428.
31. Eich, R. F., Li, T., Lemon, D. D., Doherty, D. H., Curry, S. R., Aitken, J. F., Mathews, A. J., Johnson, K. A., Smith, R. D., Phillips, G. N., Jr., and Olson, J. S. (1996) Mechanism of NO-induced oxidation of myoglobin and hemoglobin, *Biochemistry 35*, 6976−6983.
32. Yonetani, T., Tsuneshige, A., Zhou, Y., and Chen, X. (1998) Electron paramagnetic resonance and oxygen binding studies of α-nitrosyl hemoglobin. A novel oxygen carrier having no assisted allosteric functions, *J. Biol. Chem. 273*, 20323−20333.
33. Barrick, D., Ho, N. T., Simplaceanu, V., and Ho, C. (2001) Distal ligand reactivity and quaternary structure studies of proximally detached hemoglobins, *Biochemistry 40*, 3780−3795.
34. Fujii, M., Hori, H., Miyazaki, G., Morimoto, H., and Yonetani, T. (1993) The porphyrin-iron hybrid hemoglobins. Absence of the Fe−His bonds in one type of subunits favors a deoxy-like structure with low oxygen affinity, *J. Biol. Chem. 268*, 15386−15393.
35. Miyazaki, G., Morimoto, H., Yun, K. M., Park, S. Y., Nakagawa, A., Minagawa, H., and Shibayama, N. (1999) Magnesium(II) and zinc(II)-protoporphyrin IX's stabilize the lowest oxygen affinity state of human hemoglobin even more strongly than deoxyheme, *J. Mol. Biol. 292*, 1121−1136.
36. Samuni, U., Juszczak, L., Dantsker, D., Khan, I., Friedman, A. J., Perez-Gonzalez-de-Apodaca, J., Bruno, S., Hui, H. L., Colby, J. E., Karasik, E., Kwiatkowski, L. D., Mozzarelli, A., Noble, R., and Friedman, J. M. (2003) Functional and spectroscopic characterization of half-liganded iron−zinc hybrid hemoglobin: evidence for conformational plasticity within the T state, *Biochemistry 42*, 8272−8288.
37. Baldwin, J., and Chothia, C. (1979) Haemoglobin: the structural changes related to ligand binding and its allosteric mechanism, *J. Mol. Biol. 129*, 175−220.
38. Shaanan, B. (1983) Structure of human oxyhaemoglobin at 2.1 Å resolution, *J. Mol. Biol. 171*, 31−59.
39. Fermi, G., Perutz, M. F., Shaanan, B., and Fourme, R. (1984) The crystal structure of human deoxyhaemoglobin at 1.74 Å resolution, *J. Mol. Biol. 175*, 159−174.

BI049932W